



ON-LINE PSEUDO-DYNAMIC RESPONSE TEST EVALUATION OF MULTILAYER SOIL IMPROVEMENT OF LIQUEFIABLE SOILS

Naoki TAKAHASHI¹
Yoichi YAMAMOTO²
Takahiro KISHISHITA³
Masayuki HYODO⁴
Fusanori MIURA⁵
Norimasa YOSHIMOTO⁶

SUMMARY

This paper describes an on-line pseudo-dynamic response test conducted to evaluate the seismic behavior of soils improved by multilayer soil improvement. Multilayer soil improvement involves placing multiple layers of plates in a liquefiable layer and allowing the softening or liquefaction of the untreated soils between the plates so that this behavior serves to attenuate seismic motions, thereby reducing settlement and differential settlement. As a result, it was verified that untreated layers between the plates placed in multiple layers controlled the propagation of a shear wave and that multiple layers of plates were more effective than a single layer at the same ratio of improvement for attenuating seismic motions.

INTRODUCTION

Since the softening or liquefaction of soils causes significant damage during earthquakes, many soil improvement countermeasures for liquefaction have been designed to prevent this phenomenon. On the other hand, liquefaction can significantly attenuate seismic motions by enhancing the nonlinear characteristics of the soil. Liquefied soils sometimes act as a base isolation layer for superstructures, thereby reducing the harm done to structures. In the case ^{1),2)}

¹ Researcher, Sumitomo Mitsui Construction Co., Ltd, Japan, tnaoki@smcon.co.jp

² Chief Researcher, Sumitomo Mitsui Construction Co., Ltd, Japan, yoichiyamamoto@smcon.co.jp

³ Associate Researcher, FUJITA Corporation, Japan, kisisita@fujita.co.jp

⁴ Professor, Yamaguchi University, Japan, hyodo@yamaguchi-u.ac.jp

⁵ Professor, Yamaguchi University, Japan, miura@yamaguchi-u.ac.jp

⁶ Researcher, Yamaguchi University, Japan, nyoshi@yamaguchi-u.ac.jp

of spread foundation structures on reclaimed ground during the 1995 Hyogo-ken Nanbu Earthquake, for example, it was reported that the soils immediately under the spread foundation were liquefied, resulting in reduced damage to the superstructure. In the case ³⁾ of a floating foundation, it was reported that an inclination that used to exist was found to be corrected by that earthquake when the settlement behavior of the floating foundation was compared before and after the earthquake. In view of these effects, vibration-reduction technologies are now under examination that make positive use of liquefaction, including foundation forms and soil improvement methods ^{4)–7)}.

A soil improvement method that allows for the softening or liquefaction of soils is more advantageous than one that completely prevents liquefaction, both in terms of costs and the inertial forces to which a structure would be subjected. When this method is applied to spread foundation structures, however, the problem is whether settlement and differential settlement can be reduced sufficiently to meet performance requirements. Furthermore, in recent years there has been an increasing need for technologies that allow for low-cost maintenance and repair without removing the existing structures, making the applicability of countermeasure work to existing structures an important subject for study.

Thus, the authors propose a multilayer soil improvement method involving the placement of multiple layers of plate-shaped improvers to allow for softening or liquefaction of soils in order to make use of vibration-reduction effects and reduce settlement and differential settlement ^{8)–12)}. This improvement mode is based on the finding that the soft layers have a larger vibration-reduction effect when sandwiched between hard layers ¹³⁾, and it makes effective structural use of this effect. Multilayer soil improvement can be applied to soils immediately under an existing structure because improvers are constructed using a chemical feed technique.

In this study, an on-line pseudo-dynamic response test was conducted on multilayer soil improvement at various improvement ratios (total thickness of improver layers / thickness of liquefiable layers) in order to examine in detail the seismic response characteristics of this improvement mode. Further, the improvement effect of this improvement mode was examined through comparison with other improvement modes.

OVERVIEW OF THE ON-LINE PSEUDO-DYNAMIC RESPONSE TEST

Concepts of the on-line pseudo-dynamic response test

The principles of the on-line pseudo-dynamic response test are shown in Figure 1. This system, which was developed by Kusakabe et al. ¹⁴⁾, involves the following algorithm. First, the ground to be analyzed is converted into a lumped mass model into which earthquake motion is input at the base. Next, the vibration equation of the mass system is solved using a computer to determine the displacement response of each mass. The shear strain that is equivalent to the resultant displacement is applied to a specimen under computer control. The corresponding restoring force that is then automatically monitored is used to calculate the displacement response for the next step. This process is repeated for as long as the earthquake motion continues in order to directly determine the constantly changing nonlinear restoring force of the ground from the element tests. The element experiments were conducted using a simple shear test, developed by Kusakabe et al. ¹⁵⁾, Figure 2. Since testing the entire ground profile, which consisted of a number of layers, would make the system both expensive and complicated, only the ground elements that were likely to be prone to liquefaction and deformation were tested to analyze the restoring

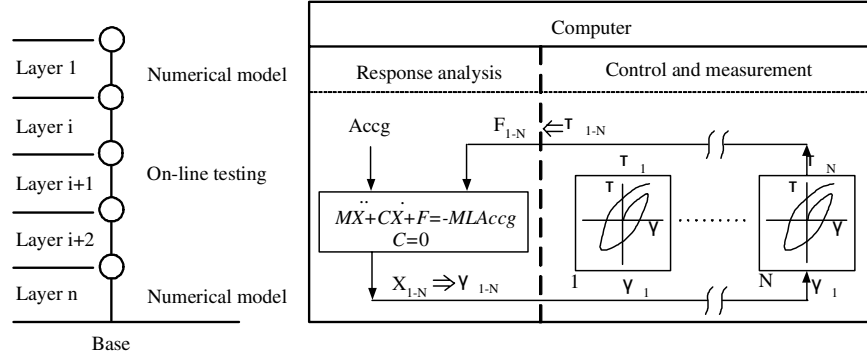


Figure 1 Conceptual diagram of on-line pseudo-dynamic response test

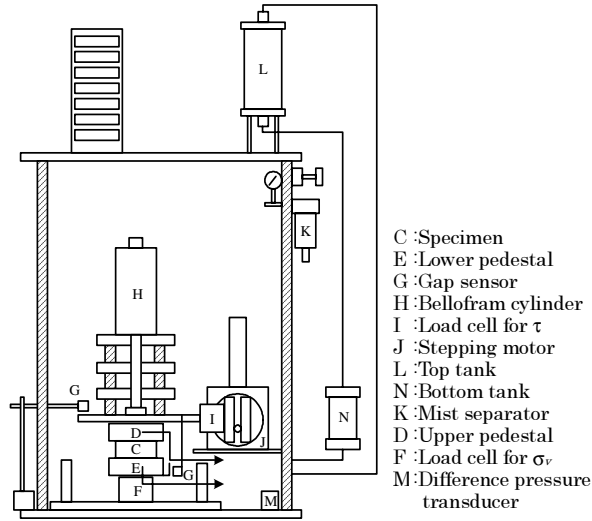


Figure 2 Simple shear testing system

force. The restoring forces of other sections were estimated numerically using modified Ramberg-Osgood models.

Analytical method

In the on-line pseudo-dynamic response test, the seismic response calculation was conducted using the following equation of motion:

$$M\ddot{X} + C\dot{X} + F = -MLA_{ccg}$$

$$C = 0$$

Where:

M is the mass matrix; C is the damping matrix; F is the restoring force vector; L is a unit vector; A_{ccg} is the input acceleration; and X is the displacement vector. The linear acceleration method was used for the initial numerical integration, and the central difference method was then used for subsequent steps.

ON-LINE PSEUDO-DYNAMIC RESPONSE TEST METHODS

Ground model

As shown in Figure 3, the model of the ground was prepared by assuming a horizontally stratified ground with a depth of 14 m and dividing the ground into seven layers, each of which was replaced by a one-dimensional mass system model. The restoring forces of layers were determined by measuring the forces in element experiments for L2 to L7 (GL-2m to GL-14m) and using modified Ramberg-Osgood models for the other layers. Layers L2 to L7 were chosen as liquefiable sand layers with relative density $D_r = 50\%$. L1 was a sand layer with $D_r = 50\%$ above the groundwater.

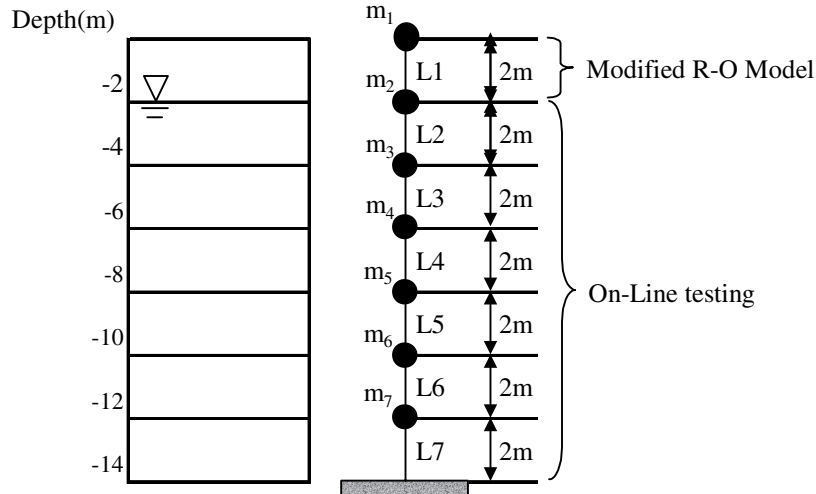


Figure 3 Gound model

Element experiments

Element tests were carried out using six sets of simple shear apparatus. Shearing was carried out under undrained conditions with zero vertical, lateral and volumetric strains. The loads were applied using stepping motors with a maximum rate of strain (0.3 %/min.) due to equipment limitations.

The soil used for the element experiments was Hamaoka Sand ($G_s=2.699$, $e_{\max}=0.933$, $e_{\min}=0.593$). Untreated specimens were prepared by pluviating Hamaoka Sand in water to a pre-determined relative density. The specimens were approximately 60 mm in diameter and 40 mm high.

Improved specimens were prepared by placing water-glass permanent grout ¹⁶⁾ in a mold and then pluviating it in water to the same relative density as the untreated specimens. These specimens were cured for 28 days in an airtight environment before being subjected to the test. Table 1 shows the standard composition of this water-glass permanent grout used in the experiment.

Table 1 Standard composition of permanent grout

	Chemical	Content (ml)
A-solution	ASF Silica	60
	Actor M	16
	Water	124
B-solution	PR Silica	60
	Water	140

Experimental and analytical conditions

The on-line pseudo-dynamic response test, as shown in Table 2, was conducted with varying improvement modes and ratios on L2 to L7, whose restoring forces were obtained through element experiments. Here, all-layer soil improvement refers to improving all the liquefiable layers and can be defined as a conventional countermeasure work; single-layer soil improvement refers to intentionally leaving an untreated layer as the base isolation layer under an improved layer⁵⁾, for which a case of design¹⁷⁾ has already been reported. In the table, a case name represents improvement mode and ratio. Since S and M represent "single-layer" and "multilayer" respectively, M050, for example, represents a case with an improvement mode of multilayer and an improvement ratio of 50%.

The analytical parameters of the L1 chosen for the modified Ramberg-Osgood models are $G_0=48697.35$ kPa, $\tau_f=22.56$ kPa, $\alpha=2.451$, $\beta=2.293$. The earthquake input waves were those observed at location PI-79mNS (maximum acceleration of 570 Gal), at a depth of 79 m on Kobe Port Island during the 1995 Hyogo-ken Nanbu Earthquake. (Figure 4)

Table 2 Test Configurations

Test case	N000	S017	S050	M033	M050	A100
Improvement ratio	0%	17%	50%	33%	50%	100%
L1	Non liquefaction layer					
L2	Untreated layer	Improved layer	Improved layer	Improved layer	Improved layer	Improved layer
L3		Untreated layer		Untreated layer	Untreated layer	
L4			Improved layer	Improved layer		
L5			Untreated layer	Untreated layer	Untreated layer	
L6				Improved layer	Improved layer	
L7		Untreated layer	Untreated layer			

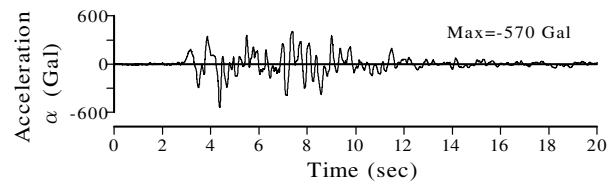


Figure 4 Input base motion

RESULTS AND DISCUSSION

Cyclic shear strength characteristic of improved sand

Figure 5 shows the relationships between N_t , the cycle count and τ/σ'_m , the ratio of cyclic shear stresses required in untreated and improved sands ($q_u=159$ kPa) to reach 5% of both amplitudes of the shear strains, which are acquired in the cyclic simple shear test using the simple shear testing system shown in Figure 2.

When comparison is made at a cycle count of 20, the improved sand has a cyclic shear strength of 1.05 and the untreated sand 0.30, demonstrating that the former has more than three times as high a cyclic shear strength as the latter. Further, the untreated sand is liquefied at a strain of 5% whereas the improved sand is not.

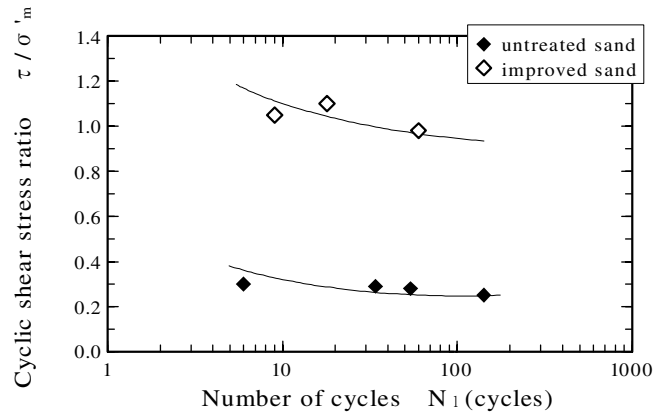


Figure 5 Relationships between the cyclic shear stress ratio and the number of cycles

Stress-strain relationships and effective stress paths

Figure 6 shows the relationships between the shear stress τ and the shear strain γ of L2 to L5, which are compared between improvement modes. Untreated layers except the underlayer, when the shear stress reaches the maximum, become liquefied and retain almost no shear stress due to sharp increases of strain. It is characteristic that this tendency is conspicuous for L5 in S050 and L3 and L5 in M050, i.e., layers immediately under an improved layer or sandwiched between improved layers. Furthermore, it is obvious from the result of A100 that each layer has a larger shear stress than in other cases. This result has caused us to infer that, in A100, each of the layers has a large restoring force and that large seismic motions propagate to upper layers.

Figure 7 shows the effective stress paths for the same case as shown in Figure 6. For the effective stress paths of sand, the phase transformation line (PTL) for Hamaoka Sand derived from the results of off-line monotonic undrained tests. Obviously, untreated layers get liquefied due to the sudden progress of deformation as soon as the PTL is exceeded. On the other hand, improved layers, although the effective stress decreases somewhat, ultimately reach a stationary state while maintaining about 70-80% of the initial effective confining pressure.

Acceleration time-history

Figure 8 shows, for the same case, the time history of response acceleration α at mass points m1 through m5. The result for N000 shows that, at mass points m1 to m4, the waveforms are attenuated with vibration and come to have longer periods. This is because the liquefaction significantly lowered the solidity of L2 to L4 and limited the propagation of seismic motions to upper layers. On the other hand, the result for A100 shows that the waveforms do not have any prolonged period at any of the mass points and that the response is large. In contrast, the result for S050 shows that the waveforms at mass points m1 to m4 are attenuated more than those in A100, demonstrating the vibration reduction effect due to the liquefaction of L5. Further, M050, despite some high-frequency elements in the waveforms at mass point m4 in the improved layer (L4), has characteristic waveforms at mass points m1 to m3 in the upper layers, that are significantly attenuated and have longer cycles, in the same way as in N000. This is because L3 becomes liquefied in addition to L5. This result, despite the fact that L2 is an improved layer, clearly shows that the liquefaction of L3 has a vibration reduction effect that extends up to the surface layer.

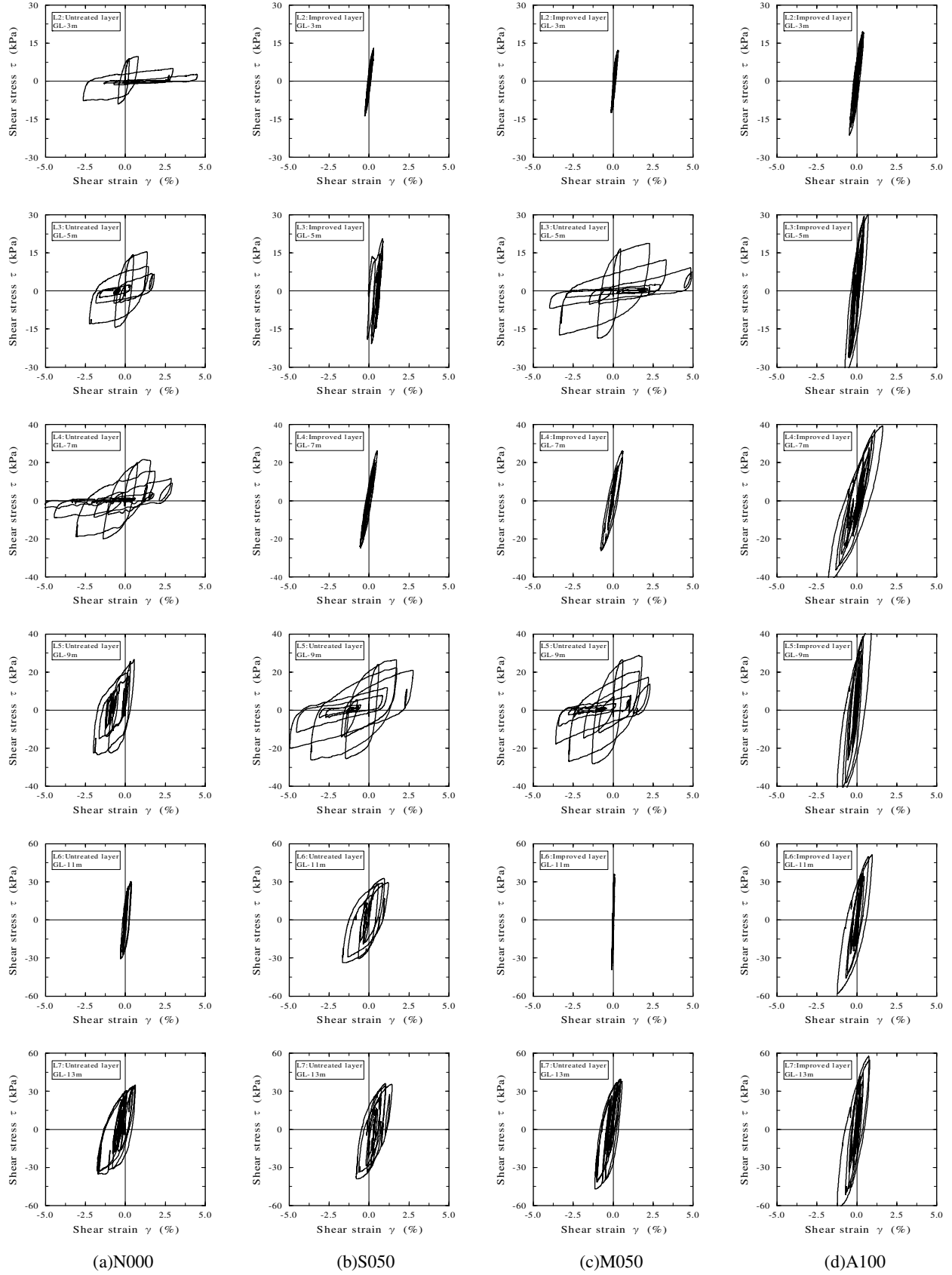
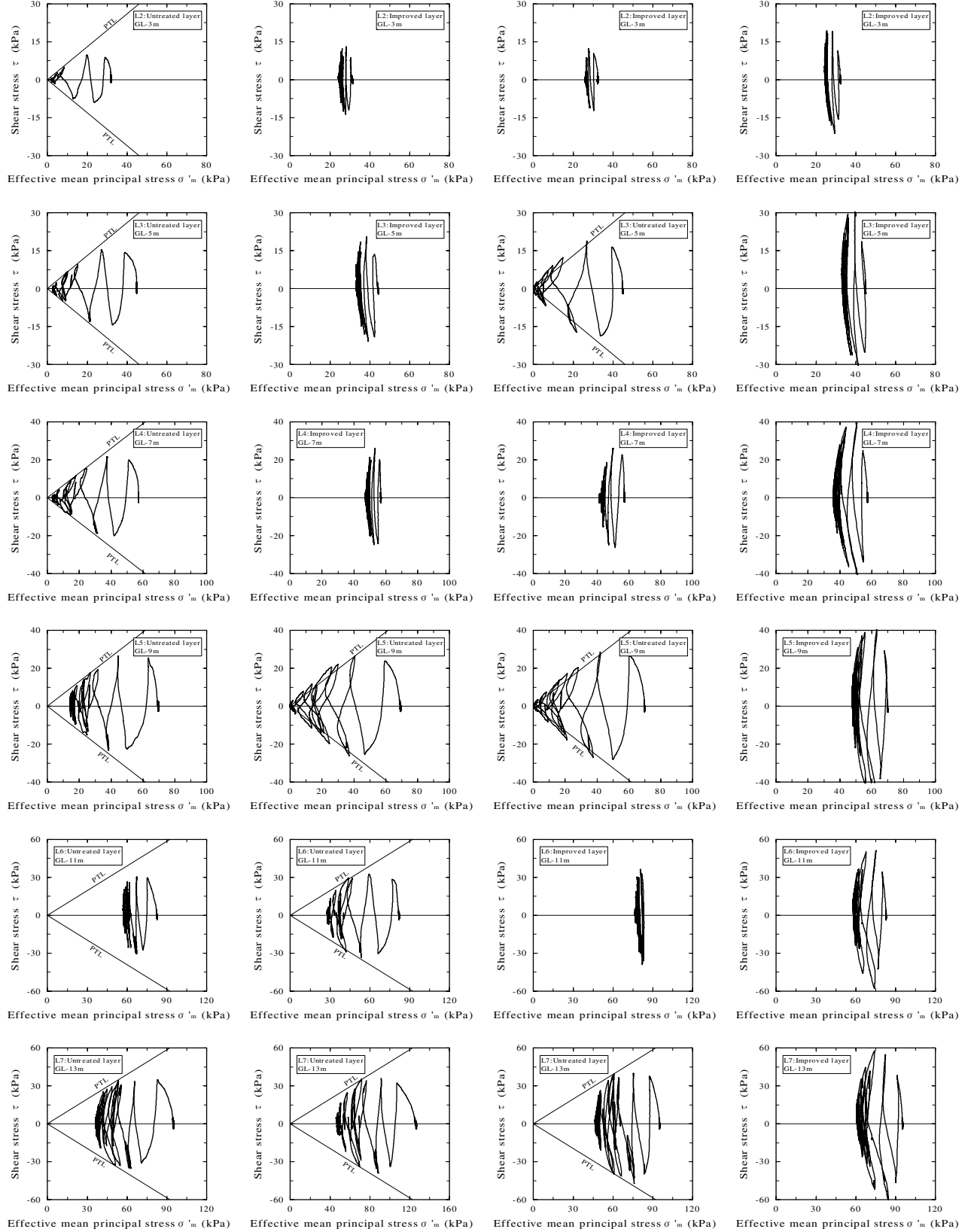


Figure 6 Relationships between shear stress τ and shear strain γ



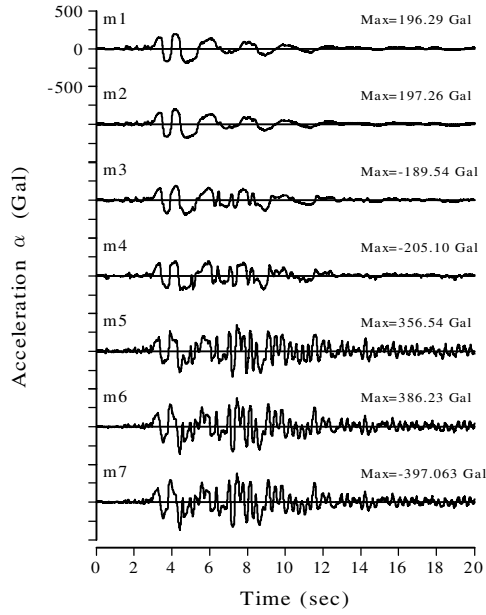
(a)N000

(b)S050

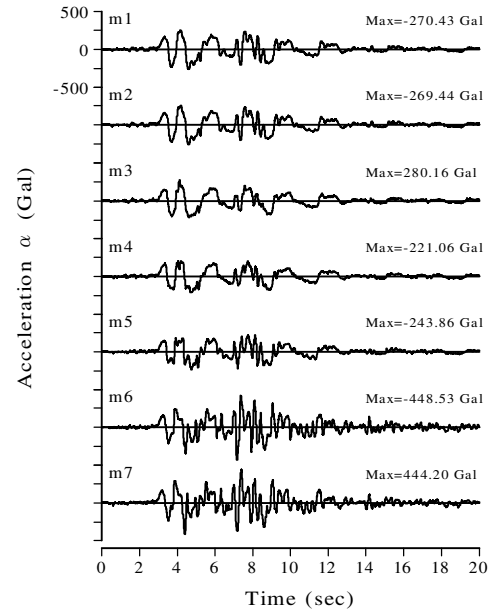
(c)M050

(d)A100

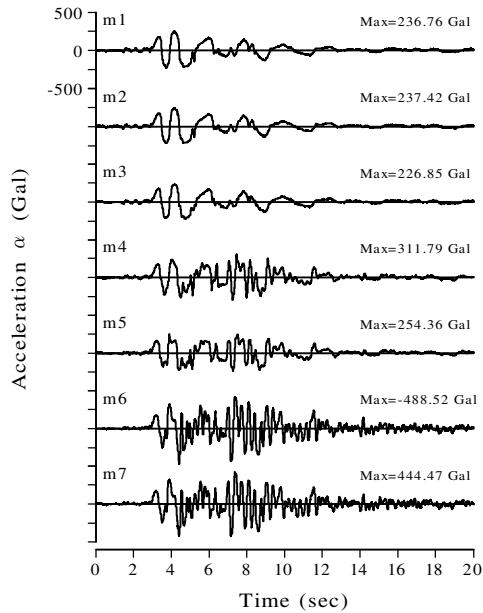
Figure 7 Effective stress paths



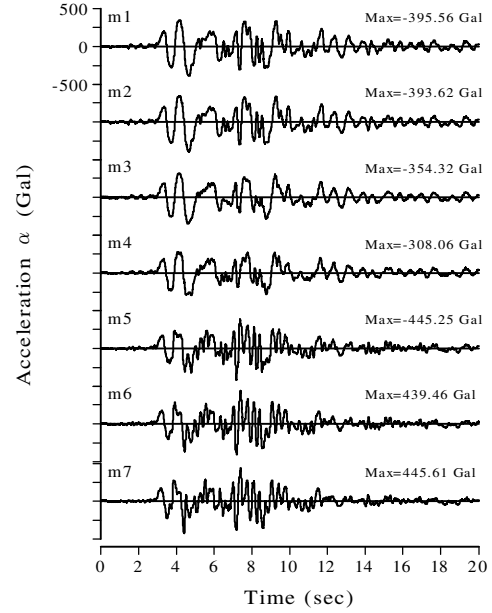
(a) N000



(b) S050



(c) M050



(d) A100

Figure 8 Acceleration time histories

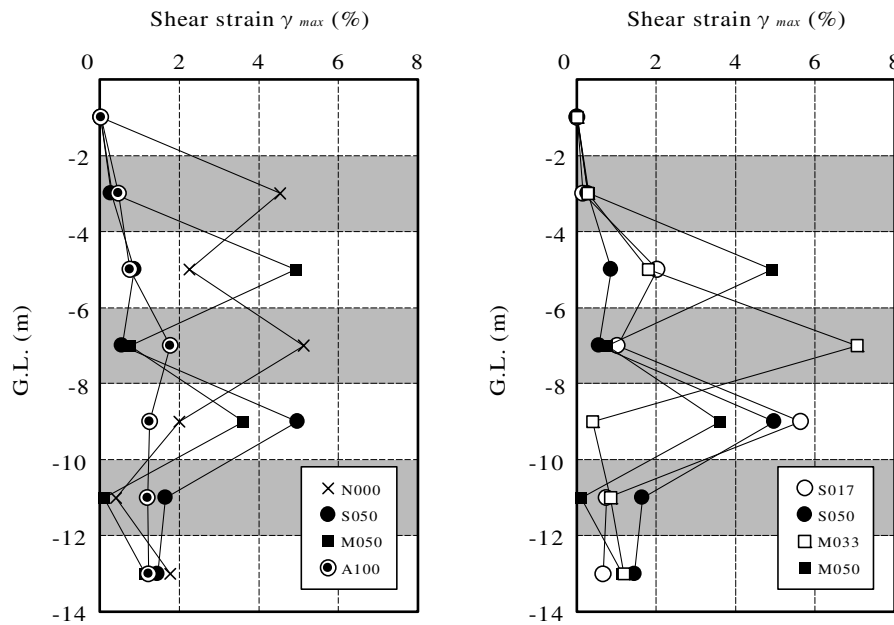
Distributions of maximum acceleration and shear strain with depth

Figures 9 and 10 show, respectively, the depth distributions of the maximum shear strain, γ_{\max} and the maximum response acceleration, α_{\max} to compare the improvement modes and ratios.

Concerning the maximum shear strain, let us look at the comparison of improvement modes shown in Figure 9(a). In N000, the strain becomes larger due to liquefaction at lesser depth than GL-10m and the

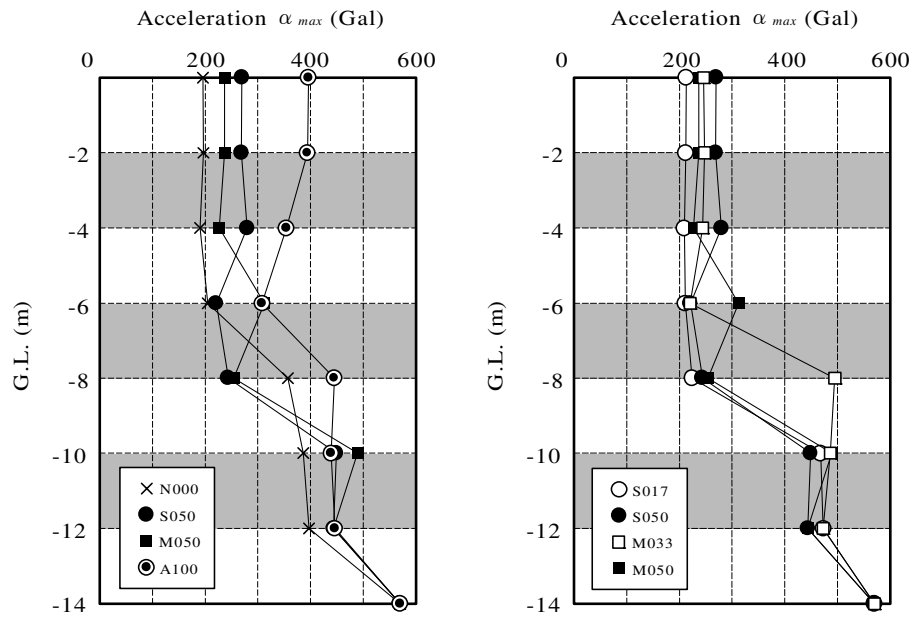
maximum value is as large as 5%. In A100, in contrast, the strain is not so large and the maximum value is 2% or less. S050 has a distribution pattern in which an untreated layer immediately under an improved layer (L5 at GL-8m to GL-10m) has a large strain. M050 has a characteristic distribution pattern in which the strain grows significantly in untreated layers sandwiched between improved layers (L3 at GL-4m to GL-6m, and L5 at GL-8m to GL-10m). Next, let us look at the comparison of improvement ratios shown in Figure 9(b). S017 and M033 have the largest strain in L5 (GL-8m to GL-10m) and L4 (GL-6m to GL-8m), respectively. Since these are the lower of continuous untreated layers, the layers with the most significant nonlinear characteristics are different from the aforementioned result with an improvement ratio of 50%. We consider that the upper untreated layers have relatively lower strains than the lower ones because the nonlinear characteristics developed in the lower part suppress the propagation of seismic motions to the upper part. However, the upper untreated layers, having as large a strain as about 2%, have also displayed nonlinear characteristics although they are not liquefied.

Concerning the maximum response acceleration, let us look at the comparison of improvement modes shown in Figure 10(a). N000 has a distribution pattern in which the liquefaction of soils suppresses the propagation of seismic motions to upper layers, which are attenuated toward the surface layer. In contrast, A100 has a distribution pattern of accelerations that are amplified at lesser depth than GL-6m. This is because, as shown in Figure 4, the solidity of soils is scarcely decreased and the restoring force is large in this case. On the other hand, S050 has a pattern in which the acceleration is attenuated in L5 (GL-8m to GL-10m), a liquefied layer, but amplified again in L3 (GL-4m to GL-6m), an improved layer. M050 has a distribution pattern in which the acceleration tends to be amplified in improved layers but greatly attenuated in an untreated layer sandwiched between the improved layers. In particular, the acceleration at mass point m4 (GL-6m) in this case is about 1.4 times as large as for that in S050 while the acceleration at mass point m3 (GL-4m) is greatly attenuated due to the vibration-reduction effect of the liquefaction of L3 (GL-4m to GL-6m), consequently making the surface response acceleration less than that in S050. Further, in the comparison of improvement ratios shown in Figure 10(b), S017 has a similar distribution pattern to N000. It is thus obvious that in the case of single-layer soil improvement, a small improvement ratio has little influence on the distribution pattern of accelerations.



(a) Comparison of improvement modes (b) Comparison of improvement ratios

Figure 9 Depth distribution of maximum shear strain γ_{max}



(a) Comparison of improvement modes (b) Comparison of improvement ratios
Figure 10 Depth distribution of maximum acceleration

Frequency characteristics of seismic response

Figure 11 shows the acceleration response spectra of surface response waves (at mass point m1) for tests N000, S050, M050 and A100. S050 shows the same tendency as A100 in that it displays a strong response near a natural period of one second and a high response in a rather short natural-period range around 0.3 to 0.4 seconds. In contrast, M050 has a smaller response than S050 in a period range less than 2.5 seconds and significant attenuation, in particular, around 0.3 to 0.4 seconds. This shows that M050 has a high vibration reduction effect in a structure with a natural-period range shorter than one second. Further, Kazama et al.¹⁸⁾ examined the influence of soft ground on the surface response in relation to ground conditions and demonstrated that a soft layer existing below the ground surface, due to its plasticity, decreases the maximum acceleration response on the ground surface but does not significantly attenuate the long-period element of vibrations. In the current test result, no difference due to the presence of a soft layer was found among the responses in a natural-period range more than 2.5 seconds.

Relationships between acceleration attenuation ratios and improvement ratios/modes

Figure 12 shows the relationships between acceleration attenuation ratios and improvement ratios. Here, the acceleration attenuation ratios are obtained by normalizing the surface maximum response accelerations of untreated and improved soils to those of A100. First, the acceleration attenuation ratio, getting smaller as the improvement ratio gets lower, is found to be 50% for untreated soils, compared with those subject to all-layer soil improvement. Further, similar comparisons reveal that the acceleration attenuation ratio is about 70% for single-layer soil improvement (with an improvement ratio of 50%) and about 60% for multilayer soil improvement (with an improvement ratio of 50%).

From these facts, it is apparent that multilayer soil improvement, i.e., placing of improvers in a way that allows for partial softening and liquefaction of soils, has a higher vibration-reduction effect than all-layer soil improvement, and even larger than single-layer soil improvement with the same improvement ratio.

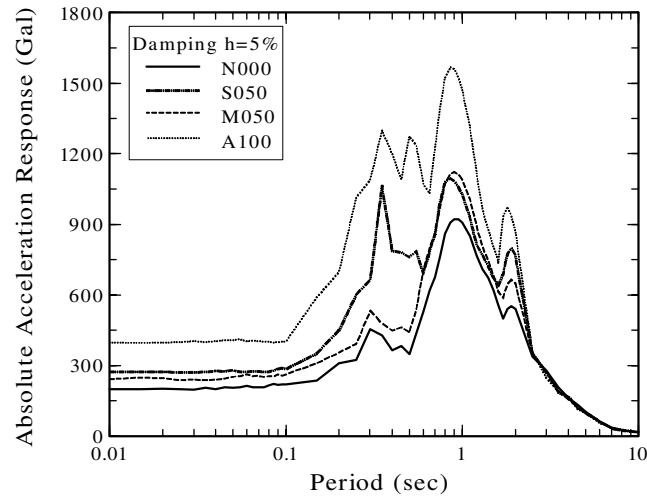


Figure 11 Comparison of acceleration spectra for surface and input wave motions

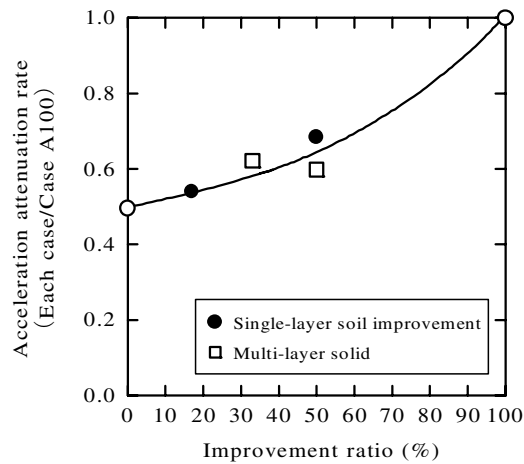


Figure 12 Relationship between acceleration attenuation rate and improvement ratio

CONCLUSIONS

This study examined the seismic response characteristics of multilayer soil improvement with an on-line pseudo-dynamic response test. Further, the improvement effect of this improvement mode was examined in comparison with other improvement modes. The following lists the findings made in this study.

- (1) It was confirmed that an untreated layer has a large vibration-reduction effect when it is located immediately under an improved layer or sandwiched between improved layers.
- (2) When compared with all-layer soil improvement, the acceleration attenuation ratio is about 70% for single-layer soil improvement (with an improvement ratio of 50%) and about 60% for multilayer soil improvement (with an improvement ratio of 50%). It was found that multilayer soil improvement has a higher vibration-reduction effect than all-layer soil improvement, which is also higher than single-layer soil improvement with the same improvement ratio.

- (3) It was confirmed that multilayer improvement has a higher vibration-reduction effect especially in a structure with a natural-period range shorter than one second.

ACKNOWLEDGEMENTS

We would like to express our gratitude to the Permanent Grout Association, which provided us with the water-glass permanent grout material that we used in this study.

REFERENCES

1. Hirai Y, Kakurai M, Maruoka M, Yamashita K, Aoki M." Behavior and evaluation of spread foundations on liquefied reclaimed artificial ground." The Foundation Engineering & Equipment, Vol.24, No.11, pp.60-66, 1996. (in Japanese)
2. Kakurai, M., Aoki, M., Hirai, M. and Matano, H. "Investigation of Spread Foundations on Liquefied Man-made Islands" The Japanese Geotechnical Society, Vol.44, No.2, pp.64-66, 1996. (in Japanese)
3. Matsuo, M., Tsuji, E., Kitagawa, M. and Ono, T. "Effect of floating foundation in the filled ground", The Foundation Engineering & Equipment, Vol.24, No.11, pp.54-59, 1996. (in Japanese)
4. Earthquake Engineering Committee. "Guidelines for structural design methods for vibration damping, base isolation and vibration control" JSCE, 2002. (in Japanese)
5. Fukutake, K. "Ground isolation due to liquefaction and its effect on structure (Part2) " Proceedings of the 36th Japan national conference on geotechnical engineering, pp.1735-1736, 2001. (in Japanese)
6. Fukutake, K. "Base isolation foundation utilizing nonlinearity of weak ground - focusing on ground base isolation by positive utilization of liquefaction" The Foundation Engineering & Equipment, Vol.30, No.12, pp.21-28, 2002. (in Japanese)
7. Fukutake, K. "Ground Isolation Technique Utilizing Liquefaction Phenomena "The Japanese Geotechnical Society, Vol.51, No.3, pp.31-33, 2003. (in Japanese)
8. Miura, F., Hyodo, M., Yoshimoto, N., Kishishita, T., Yamamoto, Y. and Takahashi, N. "Study on Multi-layer Solid of Liquefiable ground (Part1: shaking table testing), Proceedings of the 38th Japan National Conference on Geotechnical Engineering, pp. 1873-1874, 2003. (in Japanese)
9. Hyodo, M., Miura, F., Yoshimoto, N., Yamamoto, Y., Takahashi, N. and Kishishita, T. "Study on Multi-layer Solid of Liquefiable ground (Part2: effect of improvement)", Proceedings of the 38th Japan National Conference on Geotechnical Engineering, pp. 1875-1876, 2003. (in Japanese)
10. Hyodo, M., Miura, F., Yoshimoto, N., Takahashi, N., Yamamoto, Y., Kishishita, T. and Kimura, S. " Study on Multi-layer Solid of Liquefiable ground (Part 3: on-line pseudo-dynamic response test)", Proceedings of the 38th Japan National Conference on Geotechnical Engineering, pp.1877-1878, 2003. (in Japanese)
11. Miura, F., Hyodo, M., Yoshimoto, N., Kishishita, T., Yamamoto, Y. and Takahashi, N. "Shaking table test of liquefiable ground improved by multilayer soil improvement (effect of improvement ratio and improvement area)", Proceedings of the 58th Annual Conference of the Japan Society of Civil Engineering, III, pp.293-294, 2003. (in Japanese)
12. Hyodo, M., Miura, F., Yoshimoto, N., Takahashi, N., Yamamoto, Y., Kishishita, T. and Kimura, S. " On-line pseudo-dynamic response test of liquefiable ground improved by multilayer soil improvement (comparison of mode of soil improvement)", Proceedings of the 58th Annual Conference of the Japan Society of Civil Engineering, III, pp.295-296, 2003. (in Japanese)
13. Murai, N. "A study on amplification characteristics of earthquake motions in the filled ground", Journal of Structural and Construction Engineering, No.451, pp.89-98, 1993.

14. Kusakabe, S., Morio, S and Arimoto, K. "Liquefaction Phenomenon of Sand Layers by Using On-Line Computer Test Control Method", Soils and Foundations, Journal of the Japanese Society of Soil Mechanics and Foundation Engineering, Vol.30, No.3, pp.174-184, 1990.
15. Kusakabe, S., Morio, S., Okabayashi, T., Fujii, T. and Hyodo, M. "Development of a simple shear apparatus and its application to various liquefaction tests", JSCE, Journal of Geotechnical Engineering, No.617/III-46, pp.299-304, 1999. (in Japanese)
16. Yonekura, R., and Shimada, S. " Mechanism of the permanentness of permanent grout ", Civil Engineering Journal, Vol.40, No.7, pp.99-106, 1999. (in Japanese)
17. Fukutake, K., Takewaki, N., Haseba, R., Yamaguchi, H. and Yoshiwara, S. "Earthquake response simulation of foundation for the Nishida-bridge. Relocation and restoration of stone-masonry arch bridge on holocene ground, Journal of the Historical Studies in Civil Engineering, No.18, pp.395-410, 1998. (in Japanese)
18. Kazama, M., Yanagisawa, E. and Inatomi, T. "Nonliner effect of soft clay layer on the seismic response of surface ground", JSCE Journal of Geotechnical Engineering, No.575/III-40, pp.219-230, 1997. (in Japanese)